

# Lead Biosorption by Self-Immobilized *Rhizopus nigricans* Pellets in a Laboratory Scale Packed Bed Column: Mathematical Model and Experiment

Adela Kogej, Blaž Likozar and Aleksander Pavko\*

Chair of Chemical, Biochemical and Environmental Engineering, Faculty of Chemistry and Chemical Technology, University of Ljubljana, Aškerčeva cesta 5, SI-1000 Ljubljana, Slovenia

Received: December 8, 2009

Accepted: April 28, 2010

## Summary

The biosorption of lead ions from aqueous solution on a self-immobilized *Rhizopus nigricans* biomass has been studied. Experiments were performed in a laboratory scale packed bed column at different liquid flow rates and biosorbent bed heights. Recorded experimental breakthrough curves were compared to those predicted by a mathematical model, which was developed to simulate a packed bed biosorption process by a soft, self-immobilized fungal biosorbent. In the range of examined experimental conditions, the biomass characteristics such as pellet porosity and biosorption capacity substantially affected the predicted response curve. General correlations for the estimation of the intra-pellet effective diffusivity, the external mass transfer coefficient, as well as axial dispersion were successfully applied in this biological system with specific mechanical properties. Under the experimental conditions, mass transfer is controlled by the external film resistance, while the intra-pellet mass transfer resistance, as well as the effect of axial dispersion, can be neglected. A new parameter  $\alpha$ , the fraction of active biomass, with an average value of  $\alpha=0.7$ , was introduced to take into account the specific biomass characteristics, and consequently the observed non-ideal liquid flow through the bed of fungal pellets.

*Key words:* biosorption, lead, packed bed column, mathematical model, *Rhizopus nigricans*

## Introduction

The effect of toxic metals on the environment and the need for their recovery has initiated the development of cost-effective treatment technologies in the recent decades. Among them, biosorption has gained significance because it is a convenient method for the treatment of large volumes of effluents with low concentrations of pollutants. It is a fast and reversible process, which in its mechanism resembles adsorption and in some cases ion exchange, and is often performed in a packed bed column (1). Its performance can be explained by the comparative analysis of experimental and predicted breakthrough curves.

Numerous mathematical models, which enable the prediction of breakthrough curves, have been described in the literature, taking into account the biosorption kinetics, internal and external mass transfer as well as the liquid phase dynamics (axial dispersion), and are consequently able to explain the column performance. In a few studies, some simplifications were initially applied. For example, some sorption models not considering axial dispersion were used to describe biosorption, taking into account biosorption kinetics and mass transfer (2–4). A different approach using the advection-dispersion-reaction (ADR) equation was taken by Fassò (5). Here, the mass transfer resistance was neglected and local equilibrium was assumed. With the same ADR model, considering also the mass transfer resistances and introduc-

\*Corresponding author; Phone: ++386 1 241 9506; Fax: ++386 1 241 9530; E-mail: saso.pavko@fkkk.uni-lj.si

ing the overall apparent axial dispersion coefficient, which thus represented the key parameter of the model, a substantial simplification in model calculations was achieved (6). Similar approach, but a more detailed parameter analysis, was considered by some authors. For example, the corresponding parameter sensitivity analysis showed the model to be insensitive to the axial dispersion coefficient (7,8). On the other hand, it was found that the models were sensitive to biosorption kinetic constants and to the mass transfer coefficient within the biosorbent (7) or to the changes in liquid film mass transfer coefficient (8). Similarly, the studies of biosorption kinetics showed that the model was sensitive to both the external mass transfer coefficient and the pore diffusivity. Furthermore, the longitudinal dispersion coefficient also played an important role in this model (9). Biosorption process simulation tools were also presented and critically discussed (10). The complex interactions of biosorbent material properties, mass transfer and liquid flow characteristics during biosorption are thus evident from the cited literature. In those studies, mostly pretreated and rigid solid biosorbent material was investigated. Pretreatment is certainly advantageous concerning mechanical properties, but it demands additional resources. For this reason, naturally immobilized biomass in the form of pellets with good biosorption capacities is an interesting type of biosorbent. However, it is a highly porous, soft and mechanically sensitive material, and this might affect the column performance.

Recently, the biosorption and bioaccumulation of lead ions ( $Pb^{2+}$ ) by *Rhizopus arrhizus* has been studied (11–14). In some cases, the biosorption and bioaccumulation of lead ions by different Fungi, *i.e.* *Rhizopus* (12, 13), *Sporotrichum* (15), *Amanita* (16), *Aspergillus* (17,18) and *Neurospora* (19), Bacteria, like *Pseudomonas* (20) and *Streptomyces* (21), then Protista, namely *Chlorella* (22), and Plantae, explicitly *Cladophora* (23) and *Sphagnum* (24), were modelled. Modelling of the biosorption and bioaccumulation of lead ions in columns by *Rhizopus* or similar moulds is only mentioned by El-Naas *et al.* (22), yet the literature data on this topic remain rare.

The results from our previous investigation of the mechanism of lead biosorption by the self-immobilized pellets of fungus *Rhizopus nigricans* were applied in this work (25). The type of examined biomass is interesting due to its relatively high biosorption capacity and the natural form of the pellets, which facilitates the solid-liquid separation in biosorption reactors. The main goal of this research is to develop a mathematical model of the biosorption process in a packed bed column on the basis of known biosorption equilibrium data, taking into account the internal and film mass transfer resistances, the type of liquid flow, as well as the packing characteristics of the biosorbent material. Comparison with the experimental results allowed an examination of the global biosorption process rate on the basis of detailed parameter analysis, and therefore a better insight into the complex performance of the investigated reactor.

## Mathematical Model

To describe the biosorption process in a packed bed column by an adequate mathematical model, the mate-

rial balance in the liquid phase, the film mass transfer and the diffusion inside the biosorbent pellet were taken into account. Constant temperature and pH were assumed. Axial dispersed plug flow of the liquid phase was considered and the advection–dispersion–reaction equation (ADR) (6) was taken as the basic material balance equation describing biosorption in the packed bed. On the basis of our observations during the experimental work, explained in detail later through the text, a new parameter, the fraction of active biomass,  $\alpha$ , was introduced into the ADR equation so that this modification gives Eq. 1:

$$\begin{aligned} \frac{\partial C}{\partial t} &= D_{ax} \frac{\partial^2 C}{\partial z^2} - u_i \frac{\partial C}{\partial z} - \alpha \rho_{ap} \frac{(1-\varepsilon)}{\varepsilon} \frac{\partial \bar{Q}}{\partial t} \\ C(t=0) &= 0 \\ C(z=0) &= C_0 \\ \left. \frac{\partial C}{\partial z} \right|_{z=L} &= 0 \\ \bar{Q}(t=0) &= 0 \end{aligned} \quad /1/$$

The symbols in the above equation are as follows:  $C$  is the lead concentration in the liquid phase,  $C_0$  is the appropriate column input concentration,  $L$  is the height of the column,  $\varepsilon$  is packed bed porosity,  $t$  is time,  $z$  is axial distance in the packed bed,  $u_i$  is fluid linear velocity in the void space between the particles,  $\rho_{ap}$  is apparent biomass density,  $\bar{Q}$  is average lead concentration in the biomass per unit of biomass dry mass, and  $D_{ax}$  is axial dispersion coefficient.

The mass balance equation over a biosorbent particle, supposing that there is no accumulation in the fluid film around the particles, is given by Eq. 2:

$$\rho_{ap} k_p a_p (Q^* - Q) = k_f a_p (C - C^*) \quad /2/$$

Here the symbols are as follows:  $k_p$  is the particle mass transfer coefficient,  $a_p$  is specific surface area of the biosorbent particle,  $Q^*$  is the equilibrium lead concentration in the biomass,  $Q$  is the lead concentration in the biomass,  $k_f$  is the film mass transfer coefficient, and  $C^*$  is the equilibrium lead concentration in the liquid.

Taking into account the mass transfer resistance in the solid phase due to diffusion in the biosorbent pores and using the linear driving force approximation, the following mass balance can be written (26) (Eq. 3):

$$\frac{\partial \bar{Q}}{\partial t} = \frac{60 D_e}{d_p^2} (Q^* - Q) \quad /3/$$

The symbols in Eq. 3 are as follows:  $D_e$  is the effective diffusivity in the biomass and  $d_p$  is the pellet diameter.

Equilibrium between the lead concentration in the solid material  $Q^*$  and that in the liquid phase  $C^*$  is given by the Langmuir adsorption isotherm (Eq. 4):

$$Q^* = \frac{Q_{max} C^*}{K + C^*} \quad /4/$$

where  $Q_{max}$  is the maximum biosorption capacity and  $K$  is the dissociation constant.

The system of Eqs. 1 to 4 was solved numerically using the finite difference method (27) to give the theo-

retical concentration–time profiles using the condition  $\alpha=1$ . The mathematical model was then fitted to the experimental breakthrough curves obtained at different bed heights and flow rates with the fraction of active biomass,  $\alpha$ , as a fitting parameter. Furthermore, sensitivity analysis of the proposed mathematical model was performed. The influence of all model parameters (related to biomass characteristics, operating conditions and mass transfer) on the predicted breakthrough curves was investigated separately, only one parameter at a time.

## Materials and Methods

Biosorbent was prepared in the following manner: biosorbent used for experiments was a self-immobilized growth form of the fungus *Rhizopus nigricans* (ATCC 6227b) (25,28), grown in a submerged batch culture. Spherical pellets of an average diameter of  $(3.0\pm 0.5)$  mm were formed in 500-mL Erlenmeyer flasks on a rotary shaker (25,28) at 225 rpm and a temperature of 25 °C, as described elsewhere (25,28). The washed biomass was kept in suspension so that it retained its original spherical form when it was stored frozen at  $-18$  °C. Before experimental use, the biomass was defrosted and washed with deionized water.

Biosorption experiments were made in a glass column of inner diameter of  $(5.2\pm 0.1)$  cm with different heights of the packed bed of biomass pellets (20.0, 40.0, and  $55.0\pm 0.1$  cm). The biomass packed bed was formed by gently pouring the pellet suspension into the column, allowing only the excess liquid to drain from the bed at the bottom of the column. Plastic mesh was fixed at the top and the bottom of the bed to prevent wash-out of the biomass during the experiments. An additional  $(2.0\pm 0.1)$  cm layer of inert glass beads was placed at the bottom of the biomass bed to ensure a homogeneous distribution of the feed solution. A solution of  $\text{Pb}(\text{NO}_3)_2$  with an initial  $\text{Pb}^{2+}$  concentration of 100 mg/L was introduced in an upward flow *via* a peristaltic pump at flow rates from 2.5 to 10.0 mL/min. The outlet was designed as the overflow from the column. Lead ion selective electrodes (Pb 500 and R 503/P, WTW, Weilheim, Germany) were placed in the chamber just above the biomass bed to measure the outlet of  $\text{Pb}^{2+}$  concentration on-line. Additional samples were taken to verify the  $\text{Pb}^{2+}$  concentration by atomic absorption spectrometry (PerkinElmer 2280 AA spectrometer, PerkinElmer, Waltham, MA, USA). At the end of each experiment, the dry mass of the biomass packed bed was determined by drying the biomass to constant mass. No effect of shear stress on cell biosorption capacity was observed. The average values of the experimentally determined and calculated biosorbent characteristics are summarized in Table 1.

For the system under investigation, *Rhizopus nigricans* pellets and  $\text{Pb}^{2+}$  as the sorbate ions, the maximum biosorption capacity was determined to be  $Q_{\max}=83.5$  mg/g and the dissociation constant to be  $K=8.06$  mg/L. Both constants were determined based on the Langmuir biosorption isotherm (25).

The internal pellet porosity,  $\varepsilon_p$ , was determined by image analysis (29). Several representative pellets of  $(3.0\pm 0.5)$  mm in diameter were immobilized in paraffin

Table 1. Biomass characteristics used in the mathematical model

| Biomass characteristics |                        |       |
|-------------------------|------------------------|-------|
| $d_p$                   | m                      | 0.003 |
| $a_p$                   | 1/m                    | 2000  |
| $\rho_s$                | $\text{kg}/\text{m}^3$ | 1300  |
| $\rho_{ap}$             | $\text{kg}/\text{m}^3$ | 39    |
| $\varepsilon_p$         | -                      | 0.97  |
| $K$                     | $\text{g}/\text{m}^3$  | 8.05  |
| $Q_{\max}$              | $\text{g}/\text{kg}$   | 83.5  |

wax and cut with a microtome (29) into thin slices. Microscope preparations of consecutive slices of the biomass pellet were inspected and photographed under the microscope (29), then the pellet porosity was calculated from the binarized photomicrographs to be 0.97.

Because of the soft structure of the biomass, it was not possible to pack the bed with exactly the same bed porosity in each experiment. Therefore, the packed bed porosity,  $\varepsilon$ , was calculated from the known quantities measured after each experiment, assuming that the pellets were uniform nonporous spheres (Eq. 5):

$$\varepsilon = 1 - \left( \frac{m}{\rho_{ap} V_0} \right) \quad /5/$$

where  $\rho_{ap}$  is the apparent density of the biomass,  $m$  is the dry mass of the biomass and  $V_0$  is the bed volume.

The solid density of the biomass,  $\rho_s$ , was calculated from Eq. 6. The whole bed of biomass was compressed, drained and dried to constant mass under a heavy weight so that there was minimum free space inside the dried biomass. Dry mass,  $m$ , and volume,  $V_{\text{dry}}$  were measured after several experiments and the average calculated  $\rho_s$  was taken as the biomass solid density:

$$\rho_s = \frac{m}{V_{\text{dry}}} \quad /6/$$

The apparent density,  $\rho_{ap}$ , was calculated from the estimated solid density and the internal pellet porosity according to Eq. 7:

$$\rho_{ap} = \rho_s (1 - \varepsilon_p) \quad /7/$$

Only a limited number of studies have applied engineering principles of process kinetics to the biosorption, but none of them used microbial biomass with the previously described specific characteristics. Therefore, we followed generally accepted correlations to determine the mathematical model coefficients, stated in Table 2. The diffusivity inside the porous particles was assumed to be lower than the molecular diffusivity (30), as is often the case found in the literature (10). The film mass transfer coefficient,  $k_f$ , was estimated from the correlation (Eq. 8) of the flow of liquid through a packed bed of spherical particles with diameter  $d_p$  (31):

$$Sh = \frac{d_p k_f}{D_m} = \frac{1.09}{\varepsilon} Sc^{0.33} Re^{0.33} \quad /8/$$

Table 2. Working parameters and corresponding calculated coefficients used in the mathematical model

| Parameter     | Unit                   | Range                 |                       |
|---------------|------------------------|-----------------------|-----------------------|
|               |                        | Min.                  | Max.                  |
| $C_0$         | $\text{g/m}^3$         | 100                   | 100                   |
| $F_v$         | $\text{mm}^3/\text{s}$ | 41.7                  | 166.7                 |
| $L$           | m                      | 0.18                  | 0.55                  |
| $A$           | $\text{m}^2$           | $2.12 \cdot 10^{-3}$  | $2.12 \cdot 10^{-3}$  |
| $V_0$         | $\text{m}^3$           | $0.38 \cdot 10^{-3}$  | $1.18 \cdot 10^{-3}$  |
| $m$           | g                      | 4.70                  | 11.74                 |
| $\varepsilon$ | -                      | 0.68                  | 0.75                  |
| $D_m$         | $\text{m}^2/\text{s}$  | $9.45 \cdot 10^{-10}$ | $9.45 \cdot 10^{-10}$ |
| $D_e$         | $\text{m}^2/\text{s}$  | $3.0 \cdot 10^{-10}$  | $3.0 \cdot 10^{-10}$  |
| $u_0$         | $\text{m/s}$           | $2.02 \cdot 10^{-5}$  | $8.15 \cdot 10^{-5}$  |
| $u_i$         | $\text{m/s}$           | $2.72 \cdot 10^{-5}$  | $1.20 \cdot 10^{-4}$  |
| $k_f$         | $\text{m/s}$           | $1.82 \cdot 10^{-6}$  | $3.16 \cdot 10^{-6}$  |
| $D_{ax}$      | $\text{m}^2/\text{s}$  | $6.62 \cdot 10^{-8}$  | $2.08 \cdot 10^{-7}$  |

where  $Sh$  is Sherwood number, and  $Sc$  (Schmidt number) and  $Re$  (Reynolds number) are defined according to Eqs. 9 and 10:

$$Sc = \frac{\eta_L}{\rho_L D_m} \quad /9/$$

$$Re = \frac{\rho_L u_0 d_p}{\eta_L} \quad /10/$$

where  $\eta_L$  is the viscosity and  $\rho_L$  is the density of the liquid phase, while  $u_0$  is the superficial velocity.

The axial dispersion coefficient,  $D_{ax}$ , for the liquid flow,  $F_v$ , through a packed bed of porous particles in a column with cross section,  $A$ , was calculated using the Wakao's correlation (31) (Eq. 11):

$$D_{ax} = \frac{20D_m}{\varepsilon} + \frac{d_p F_v}{2\varepsilon A} \quad /11/$$

### Results and Discussion

Based on the estimated parameters and experimental operating conditions (Tables 1 and 2), the model was solved numerically to give the theoretical breakthrough curves. The direct numerical solution of the model ( $\alpha=1$ ) showed a correct tendency of the mathematical model in which a satisfying agreement of the mathematical model and experimental data was found. However, a certain disagreement of the non-fitted model with the experimental data was observed.

In the next step, the mathematical model was fitted to the experimental data with the fraction of active biomass,  $\alpha$ , as a fitting parameter (Fig. 1). This parameter, the fraction of active biomass,  $\alpha$ , accounts for all irregularities within the packed bed which appeared due to the physical characteristics of the biosorbent and the consequent non-ideal packed bed conditions. Although we attempted to achieve maximal consistency during the packing procedure, the individual column packing was not completely uniform and beds also differed from

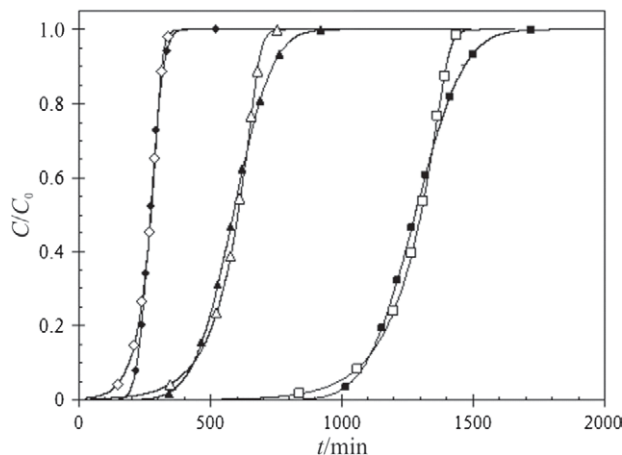


Fig. 1. Agreement of the mathematical model with one fitting parameter, the fraction of active biomass,  $\alpha$ , with the experimental breakthrough curves for the column height  $L=20$  cm and flow rates  $F_v=2.5-10.0$  mL/min (experimental values: ■ 2.5 mL/min, ▲ 5.0 mL/min and ◆ 10.0 mL/min; fitted values: □ 2.5 mL/min, △ 5.0 mL/min and ◇ 10.0 mL/min)

one experiment to another. On average, the value of  $\alpha$  was always less than one, meaning that the total capacity of the column, which is dependent on the biosorption equilibrium, was never achieved. The dynamic capacity of the packed bed was in all cases lower than the equilibrium biosorption capacity. No strong correlation was found between the agreement of the model and experiment with the operating conditions (height of the column,  $L$ , and column flow rate,  $F_v$ ), as is also evident from the random and broad distribution of fitting parameter values,  $\alpha$ , shown in Table 3. Roughly speaking, with higher columns, lower fractions of active biomass,  $\alpha$ , were determined, which is consistent with the fact that higher packed beds were less uniform and worse packed.

Table 3. The average fractions of active biomass,  $\alpha$ , determined as a fitting parameter of the mathematical model

|            | $F_v=41.7 \text{ mm}^3/\text{s}$ | $F_v=83.3 \text{ mm}^3/\text{s}$ | $F_v=166.7 \text{ mm}^3/\text{s}$ |
|------------|----------------------------------|----------------------------------|-----------------------------------|
| $L=0.20$ m | 0.81                             | 0.87                             | 0.55                              |
| $L=0.40$ m | 0.70                             | 0.58                             | 0.52                              |
| $L=0.55$ m | 0.68                             | 0.62                             | 0.64                              |

The fraction of active biomass,  $\alpha$ , determined from the best fit of the model to the experimental data, was found to be in the range from 0.5 to 0.9 and the average value was around 0.7. This means that the biomass packed in the bed up to 70 % was exploited on average, when saturation of the column was complete according to the experimentally measured outlet  $\text{Pb}^{2+}$  concentration.

A parameter sensitivity study of the mathematical model was performed, where a detailed analysis of the relation between the mathematical model, the biomass properties and operating conditions was studied. During this analysis only one parameter was varied at a time, the others being set at the estimated values as presented in Tables 1 and 2.

The results of the parameter analysis are represented graphically in terms of the influence of the relative change of each parameter ( $\Delta\text{parameter}/\text{parameter}$ ) on the relative change of the mathematical model breakthrough time ( $\Delta t_{0.05}/t_{0.05}$ ) (Figs. 2 and 3).

The influence of biomass properties on the breakthrough time is shown in Fig. 2. The model is extremely sensitive to the pellet porosity. A minor decrease in its value causes a great reduction of breakthrough time. Decreased pellet porosity (from the estimated value of 0.96 to the minimal value of 0.8) could deteriorate the intra-particle mass transfer and therefore reduce the breakthrough time. The extreme response can also be attributed to the consequently increased bed porosity (according to Eqs. 5 and 7), resulting in an enhanced flow through the packed bed. The maximum biosorption capacity has the expected substantial effect on the breakthrough time. An increase of the maximum biosorption capacity pro-

portionally increases the bed capacity and consequently prolongs the breakthrough time. Pellet diameter has the opposite effect; larger pellets cause earlier breakthrough, probably due to an increased intra-particle mass transfer resistance or the larger amount of biomass inside the pellets, which thus become ineffective.

The maximum biosorption capacity, biosorbent density and void degree are the most relevant factors that influence the fixed bed reactor efficiency (5). Substantial effect of bed void fraction and particle size is also reported (8). It is also suggested that the effect of sorbent aging and consequently the loss of capacity during biosorption could be incorporated into the fixed bed model (32). These results are consistent with our findings about the substantial effect of biosorption capacity on model sensitivity and our attempt to explain this effect by an inactive fraction of biomass.

The operating conditions also have a significant influence on the breakthrough time, as is shown in Fig. 3. Increased bed porosity, liquid flow rate and initial  $\text{Pb}^{2+}$  concentration decrease the breakthrough time. The decrease of bed porosity (utilizing the same mass of biosorbent) affects the liquid velocity through the bed of particles and therefore causes earlier breakthrough times. The initial  $\text{Pb}^{2+}$  concentration and the breakthrough time are interrelated through the rate of biosorption. At the same biosorption rate, a higher initial  $\text{Pb}^{2+}$  concentration causes an earlier breakthrough time because of the inability of the biosorbent to take up more solute ( $\text{Pb}^{2+}$ ) within the same time span. On the contrary, lower initial  $\text{Pb}^{2+}$  concentrations increase breakthrough times. The quantity of biosorbent in the bed has the opposite effect on the breakthrough time. Lower biomass content causes almost proportionally earlier breakthrough because of the lower capacity of the column.

The influence of the model coefficients, directly connected to the transport regime in the observed system, on the breakthrough curves is represented in Figs. 4-6. The influence of the effective diffusivity,  $D_e$ , the film mass transfer coefficient,  $k_f$ , and the axial dispersion coefficient,  $D_{ax}$ , was studied theoretically, independent of the other biomass and operating characteristics. It can be seen that mass transfer coefficients substantially affect the response

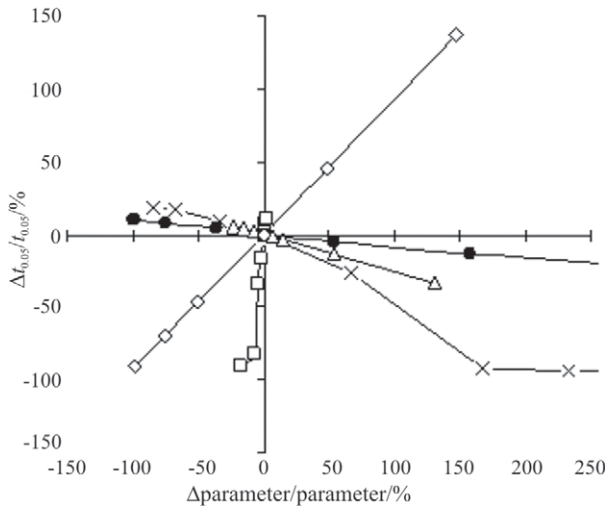


Fig. 2. Effect of the relative change of biomass characteristics on the relative change of the model breakthrough time,  $t_{0.05}$  ( $\times d_p$ ,  $\square K$ ,  $\diamond Q_{max}$ ,  $\triangle \rho_s$ )

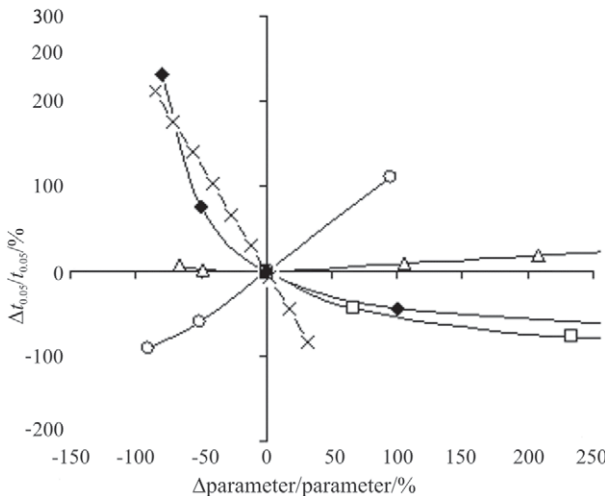


Fig. 3. Effect of the relative change of operating conditions on the relative change of the model breakthrough time,  $t_{0.05}$  ( $\times \epsilon$ ,  $\square F_v$ ,  $\circ C_0$ ,  $\triangle L$ ,  $\diamond m$ )

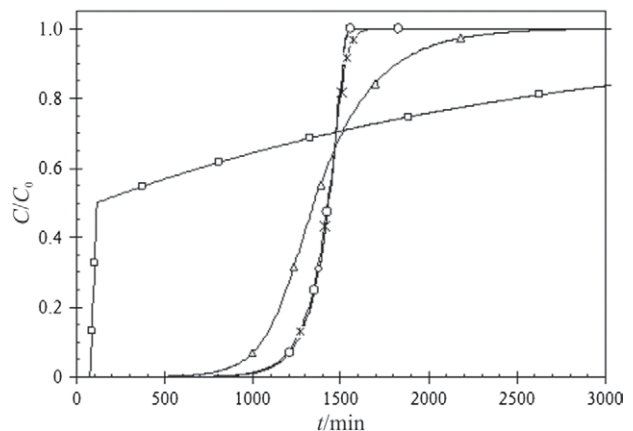


Fig. 4. Sensitivity analysis of the mathematical model: the influence of the effective diffusivity,  $D_e$  ( $\square D_e=10^{-12} \text{ m}^2/\text{s}$ ,  $\triangle D_e=10^{-11} \text{ m}^2/\text{s}$ ,  $\circ D_e=10^{-10} \text{ m}^2/\text{s}$ ,  $\diamond D_e=10^{-9} \text{ m}^2/\text{s}$ ,  $\times D_e=10^{-7} \text{ m}^2/\text{s}$ )

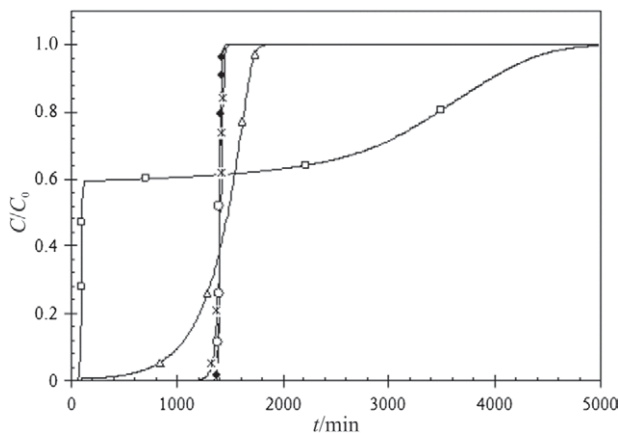


Fig. 5. Sensitivity analysis varying the film mass transfer coefficient,  $k_f$  ( $\square$   $k_f=10^{-7}$  m/s,  $\triangle$   $k_f=10^{-6}$  m/s,  $\times$   $k_f=10^{-5}$  m/s,  $\circ$   $k_f=10^{-4}$  m/s,  $\diamond$   $k_f=10^{-3}$  m/s)

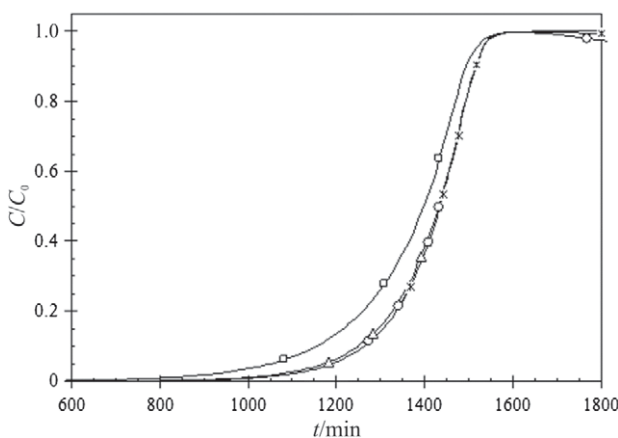


Fig. 6. Sensitivity analysis varying the axial dispersion coefficient,  $D_{ax}$  ( $\circ$   $D_{ax}=10^{-11}$  m<sup>2</sup>/s,  $\times$   $D_{ax}=10^{-9}$  m<sup>2</sup>/s,  $\triangle$   $D_{ax}=10^{-7}$  m<sup>2</sup>/s,  $\square$   $D_{ax}=10^{-6}$  m<sup>2</sup>/s)

of the mathematical model. Apart from that, the model analysis confirmed the appropriate range of the estimated relevant coefficients.

The low effective diffusivity ( $D_e < 10^{-10}$  m<sup>2</sup>/s) indicates a restricted intraparticle mass transfer and consequently enhances breakthrough times (Fig. 4). The estimated value of the effective diffusivity,  $D_e = 3 \cdot 10^{-10}$  m<sup>2</sup>/s, used in the model calculations, is shown to be within the range of no impact on the experimental system.

Different effects of internal diffusion were found in the literature. It can play an important role (7,9) or it does not influence the simulation results (8).

The influence of the film mass transfer coefficient,  $k_f$ , on the model is shown in Fig. 5. A satisfactorily high  $k_f > 10^{-5}$  m/s gives a response of the model to a step change in the packed-bed reactor almost equal to the theoretical one. However, a lower  $k_f$  omits the mass transport through the film layer around the biomass particles and therefore causes earlier breakthrough. In the experimental working range of process parameters, where  $k_f$  values were estimated to be around 2 to  $3 \cdot 10^{-6}$  m/s, the model shows a certain sensitivity. A value of  $k_f$  less than

ten times lower could already affect the system drastically, as is shown in Fig. 5, while a less than ten times higher value of  $k_f$  would no longer affect the system.

Several reports about the film transport resistance are found in the literature. For example, the model was sensitive to changes in mass transfer coefficient, when it is in the range of values of 5 to  $9 \cdot 10^{-5}$  m/s (8). The values of this coefficient of the order of magnitude of  $10^{-7}$  m/s substantially affect the model predictions (9), which is in agreement with our results. Certain sensitivity to mass transfer is also reported elsewhere (7).

Sensitivity analysis of the axial dispersion coefficient,  $D_{ax}$  (Fig. 6) shows that the effect of the axial dispersion coefficient becomes significant above  $10^{-7}$  m<sup>2</sup>/s. The estimated values of  $D_{ax} = 6 \cdot 10^{-8}$  to  $2 \cdot 10^{-7}$  m<sup>2</sup>/s, which correspond to the actual working conditions, imply that the axial dispersion coefficient does not have a significant effect on the system.

Similarly, the model is sensitive to axial dispersion coefficient if its value of  $1.2 \cdot 10^{-7}$  m<sup>2</sup>/s is multiplicatively/divisionally varied in order of  $10^3$  (7). Higher values than  $4 \cdot 10^{-5}$  m<sup>2</sup>/s would cause earlier breakthrough due to dispersion and advection. At the same time, lower value can result in the steeper curves (9).

The influence of the main model fitting parameter, the fraction of active biomass,  $\alpha$ , was also studied. This shows a great impact on the model breakthrough time, as is represented in Fig. 7. The response of the model is reasonable because the activity of the biomass is directly related to the column capacity and to the breakthrough time.

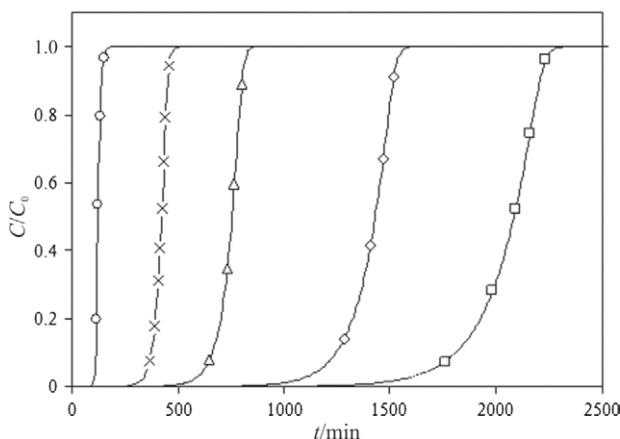


Fig. 7. Influence of the fraction of active biomass,  $\alpha$ , on the theoretical response curve ( $\circ$   $\alpha=0.025$ ,  $\times$   $\alpha=0.250$ ,  $\triangle$   $\alpha=0.500$ ,  $\diamond$   $\alpha=1.000$ ,  $\square$   $\alpha=1.500$ )

The parameter  $\alpha$  is a measure of the biomass packed bed exploitation and as such should vary between 0 and 1. Values of  $\alpha > 1$  could also be obtained as a result of the comparison between experimental and predicted results, but only as an indication of the incorrectly estimated model parameters. This can easily happen for example if the total biosorption equilibrium capacity of the biomass is underestimated. It is well known that pH influences metal uptake by the biomass. The usual procedure for the determination of the maximum biosorp-

tion capacity is the equilibrium experiment, while in the continuous flow experiments, the pH conditions might differ substantially. Furthermore, the actual  $Q_{\max}$  might be higher than that estimated due to the biomass variability, despite its careful preparation.

The agreement of the model with the experimental results is satisfactory (Fig. 1). Some deviations from the model were observed, which could be ascribed to the poorly defined biological system whose characteristics deviate from the classical chemical engineering systems of packed beds of rigid spherical porous particles. The particles are not spheres of equal size but are soft structures of intertwining hyphae, which easily adhere and form agglomerates or are compressed by gravity or due to the flow pressure. Consequently, the formation of channels and zones of unused biomass within the bed was inevitable. In addition, the actual very high pellet porosity ( $\varepsilon_p=0.96$ ) differs from the usual solid particle porosity.

## Conclusions

A mathematical model based on exact engineering principles was successfully applied to the biosorption of lead ions where essentially untreated waste fungal biomass was used as a biosorbent in a packed bed column. To take into account the specific physical properties of the biomass and consequently the observed non-ideal liquid flow through the bed of fungal pellets, a new parameter, the fraction of active biomass,  $\alpha$ , was introduced. With this modification of the model, a good agreement with the experimental results was obtained and an average value of  $\alpha=0.7$  was determined. Agreement with the model is expected to be higher in bigger reactors, where the particle to reactor diameter ratio is favourable and the packing quality is higher. Some adjustments like strengthening the biomass consistency might also solve this problem.

The comparison of simulated and experimental breakthrough curves enabled a better insight into the problem. In a detailed analysis of the mathematical model, biomass properties, operating conditions and mass transfer parameters were studied separately. It was shown that the key parameters of packed bed biosorption are the biosorbent characteristics and the operating parameters: pellet porosity, bed porosity, maximal biosorption capacity, biosorbent, lead ion concentration and flow rate.

The intra-pellet effective diffusivity, the external mass transfer coefficient and the axial dispersion coefficient were estimated using general correlations. It was shown that the obtained values describe the processes in this specific biological system reasonably well. The overall rate of biosorption is controlled by the external film resistance, while the intra-pellet mass transfer resistance, as well as the axial dispersion, can be neglected.

## Acknowledgements

Authors wish to thank Prof Dr Iztok Golobič and Dr Erik Pavlovič for their help. This work was supported by the Ministry of Higher Education, Science and Technology of the Republic of Slovenia (Research Program P2-0191 and Project L2-1501).

## References

1. D. Kratochvil, B. Volesky, Advances in the biosorption of heavy metals, *Trends Biotechnol.* 16 (1998) 291–300.
2. B. Volesky, I. Prasetyo, Cadmium removal in a biosorption column, *Biotechnol. Bioeng.* 43 (1994) 1010–1015.
3. Z. Zulfadhly, M.D. Mashitah, S. Bhatia, Heavy metals removal in fixed-bed column by the macro fungus *Pycnoporus sanguineus*, *Environ. Pollut.* 112 (2001) 463–470.
4. Y. Sag, Y. Aktay, Application of equilibrium and mass transfer models to dynamic removal of Cr(VI) ions by chitin in packed column reactor, *Process Biochem.* 36 (2001) 1187–1197.
5. A. Fassò, A. Esposito, E. Porcu, A.P. Reverberi, F. Vegliò, Statistical sensitivity analysis of packed column reactors for contaminated wastewater, *Environmetrics*, 14 (2003) 743–759.
6. A. Hatzikioseyan, M. Tsezos, F. Mavituna, Application of simplified rapid equilibrium models in simulating experimental breakthrough curves from fixed bed biosorption reactors, *Hydrometallurgy*, 59 (2001) 395–406.
7. E.A. da Silva, E.S. Cossich, C.R.G. Tavares, L.C. Filho, R. Guirardello, Modeling of copper(II) biosorption by marine alga *Sargassum* sp. in fixed-bed column, *Process Biochem.* 38 (2002) 791–799.
8. N. Abdel-Jabbar, S. Al-Asheh, B. Hader, Modeling, parametric estimation, and sensitivity analysis for copper adsorption with moss packed-bed, *Separ. Sci. Technol.* 36 (2001) 2811–2833.
9. J.P. Chen, L. Wang, Characterization of metal adsorption kinetic properties in batch and fixed-bed reactors, *Chemosphere*, 54 (2004) 397–404.
10. B. Volesky, Biosorption process simulation tools, *Hydrometallurgy*, 71 (2003) 179–190.
11. S. Bhattacharyya, T.K. Pal, A. Basumajumdar, Effect of some complex nutrients on improvement of bioaccumulation of lead by *Rhizopus arrhizus*, *J. Ind. Chem. Soc.* 86 (2009) 749–752.
12. M. Alimohamadi, G. Abolhamd, A. Keshtkar, Pb(II) and Cu(II) biosorption on *Rhizopus arrhizus* modeling mono- and multi-component systems, *Miner. Eng.* 18 (2005) 1325–1330.
13. G. Naja, C. Mustin, J. Berthelin, B. Volesky, Lead biosorption study with *Rhizopus arrhizus* using a metal-based titration technique, *J. Colloid Interface Sci.* 292 (2005) 537–543.
14. A. Basumajumdar, S. Bhattacharyya, T.K. Pal, Some trace elements enhance biosorption of lead by *Rhizopus arrhizus*, *J. Ind. Chem. Soc.* 81 (2004) 410–412.
15. Y. Tunali, H. Karaca, T. Tay, M. Kivanc, G. Bayramoglu, Biosorption of Pb(II) from aqueous solutions by a fungal biomass in a batch system: Equilibrium and kinetic studies, *Asian J. Chem.* 21 (2009) 6015–6028.
16. A. Sari, M. Tuzen, Kinetic and equilibrium studies of biosorption of Pb(II) and Cd(II) from aqueous solution by macrofungus (*Amanita rubescens*) biomass, *J. Hazard. Mater.* 164 (2009) 1004–1011.
17. T. Akar, S. Tunali, Biosorption characteristics of *Aspergillus flavus* biomass for removal of Pb(II) and Cu(II) ions from an aqueous solution, *Bioresour. Technol.* 97 (2006) 1780–1787.
18. A.Y. Dursun, A comparative study on determination of the equilibrium, kinetic and thermodynamic parameters of biosorption of copper(II) and lead(II) ions onto pretreated *Aspergillus niger*, *Biochem. Eng. J.* 28 (2006) 187–195.
19. I. Kiran, T. Akar, S. Tunali, Biosorption of Pb(II) and Cu(II) from aqueous solutions by pretreated biomass of *Neurospora crassa*, *Process Biochem.* 40 (2005) 3550–3558.
20. R.M. Gabr, S.H.A. Hassan, A.A.M. Shoreit, Biosorption of lead and nickel by living and non-living cells of *Pseudomonas aeruginosa* ASU 6a, *Int. Biodeter. Biodegr.* 62 (2008) 195–203.

21. A. Selatnia, A. Boukazoula, N. Kechid, M.Z. Bakhti, A. Chergui, Y. Kerchich, Biosorption of lead (II) from aqueous solution by a bacterial dead *Streptomyces rimosus* biomass, *Biochem. Eng. J.* 19 (2004) 127–135.
22. M.H. El-Naas, F. Abu Al-Rub, I. Ashour, M. Al Marzouqi, Effect of competitive interference on the biosorption of lead (II) by *Chlorella vulgaris*, *Chem. Eng. Process: Process Intens.* 46 (2007) 1391–1399.
23. L. Deng, Y. Su, H. Su, X. Wang, X. Zhu, Biosorption of copper (II) and lead (II) from aqueous solutions by nonliving green algae *Cladophora fascicularis*: Equilibrium, kinetics and environmental effects, *Adsorption*, 12 (2006) 267–277.
24. Y. Zhang, C. Banks, The interaction between Cu, Pb, Zn and Ni in their biosorption onto polyurethane-immobilised *Sphagnum* moss, *J. Chem. Tech. Biotechnol.* 80 (2005) 1297–1305.
25. A. Kogej, A. Pavko, Comparison of *Rhizopus nigricans* in a pelleted growth form with some other types of waste microbial biomass as biosorbents for metal ions, *World J. Microbiol. Biotechnol.* 17 (2001) 677–685.
26. R.T. Yang: *Gas Separation by Adsorption Processes, Vol. 1*, Imperial College Press, London, UK (1997) pp. 141–201.
27. J.B. Riggs: *An Introduction to Numerical Methods for Chemical Engineers*, Texas Tech University Press, Lubbock, TX, USA (1994) pp. 241–305.
28. A. Kogej, A. Pavko, Laboratory experiments of lead biosorption by self-immobilized *Rhizopus nigricans* pellets in the batch stirred tank reactor and the packed bed column, *Chem. Biochem. Eng. Q.* 15 (2001) 75–79.
29. A. Kogej, A. Pavko, Mathematical model of lead biosorption by *Rhizopus nigricans* pellets in a laboratory batch stirred tank, *Chem. Biochem. Eng. Q.* 18 (2004) 29–35.
30. P. Vanysek: Ionic Conductivity and Diffusion at Infinite Dilution. In: *CRC Handbook of Chemistry and Physics*, D.R. Lide (Ed.), CRC, Boca Raton, FL, USA (2008) pp. 5-76.
31. D.M. Ruthven: *Principles of Adsorption and Adsorption Processes*, John Wiley&Sons, New York, NY, USA (1984) pp. 212–215.
32. D. Kratochvil, B. Volesky, G. Demopoulos, Optimizing Cu removal/recovery in a biosorption column, *Water Res.* 31 (1997) 2327–2339.